Materials Research Bulletin 98 (2018) 194–199

Contents lists available at ScienceDirect

Materials Research Bulletin

journal homepage: www.elsevier.com/locate/matresbu

Large-scale synthesis of Bi_2S_3 nanorods and nanoflowers for flexible near-infrared laser detectors and visible light photodetectors

Junfeng Chao[a,*], Shumin Xing[b], Zhendong Liu[b,**], Xiutai Zhang[a], Yuliang Zhao[b], Luhua Zhao[a], Qiufeng Fan[a]

[a] College of Electronic Information and Electric Engineering, Anyang Institute of Technology, Anyang 455000, PR China
[b] College of Mathematics and Physics, Anyang Institute of Technology, Anyang 455000, PR China

ARTICLE INFO

Keywords:
Optoelectronics
Laser detector
Photodetector
Photoconductivity

ABSTRACT

Rod-like and flower-like bismuth sulphide semiconductor nanomaterials were large-scale synthesized and applied for flexible near-infrared laser detectors and visible light photodetectors. The nanorod-based flexible laser detectors have high photoresponse characteristics to 808 nm and 980 nm laser light, and their switching ratio were calculated to be 9.2 and 23.6 times, respectively. The flexible laser detectors exhibit good linear current characteristics, photo-sensitivity dependence of light intensity. Especially, the flexible nanorod-based photodetector has high LDR (linear dynamic range) value of 19.60 dB. Furthermore, the Bi_2S_3 nanorods based visible light photodetector exhibits higher LDR value than other Bi_2S_3 based photodetectors.

1. Introduction

Bismuth sulfide (Bi_2S_3), a V_2–VI_3 binary chalcogenide semiconductor, is one of the promising absorber materials worthy of exploration. With a reasonable bandgap of 1.3 ~ 1.7 eV and a high absorption coefficient near $10^5\ cm^{-1}$, it can absorb almost the entire visible light and near-infrared range of the solar spectrum [1–11]. For instance, Tang's group showed that Bi_2S_3 act as the absorber layer for thin film photovoltaics has 0.75% power conversion efficiency [12]. Bi_2S_3-Au heterostructures show superior activity for the photo degradation of MB dye [13]. Solution-processed Bi_2S_3 nanorods photodetectors are of interest in visible and near-infrared light application [14].

Among all the micro- and nanoscale devices, the laser detectors are critical for applications as binary switches in optical communications and imaging techniques, as well as in future memory storage and high performance photodetectors. Very recently, considerable efforts have been devoted to fabricating low-cost, small size, high efficiency and flexible optoelectronics devices [15–20]. Here, the simple synthesis of Bi_2S_3 nanorods and nanoflowers from one-step, large-scale, facile polyol refluxing process was realized, and we successfully fabricated high performance Bi_2S_3-based 808 nm and 980 nm near-infrared laser detectors and visible light photodetectors. Besides, the Bi_2S_3 nanorods based visible light photodetector exhibits higher LDR value than other Bi_2S_3 based flexible photodetectors. Our route here may open up a new opportunity to fabricate laser detector of other wavelengths and extend their application based on the low-cost, environmentally friendly, and high-yield mass production strategy.

2. Experimental section

All regents were purchased and used without further purification.

2.1. Synthesis of the precursor $Bi(DDTC)_3$

An equimolar mixture of analytical grade bismuth chloride ($BiCl_3$) and Sodium diethyldithiocarbamate trihydrate (DDTC) were dissolved in a mixture of water in a 100 mL beaker. After stirring for 30 min, the precursor precipitate were filtered, washed with distilled water for several times, dried in vacuum at 60 °C for 3 h.

2.2. Synthesis of Bi_2S_3 nanorods and nanoflowers

In a typical process, Bi_2S_3 nanorods were synthesized via a facile polyol refluxing process. 2 mmol of precursor $Bi(DDTC)_3$ were put into 50 mL ethylene glycol in a 250 mL three-neck flask. After stirring for 10 min, 6 mL ethylenediamine was a drop at a time into the previous solution. The reaction system was heated and kept at 190 °C for 3 h. After cooling to room temperature slowly, the brown-black product was washed with deionized and ethanol several times. The Bi_2S_3

* Corresponding author.
** Corresponding author at: College of Mathematics and Physics, Anyang Institute of Technology, Anyang 455000, PR China.
E-mail addresses: chchjjff@163.com (J. Chao), lzd200611@126.com (Z. Liu).

http://dx.doi.org/10.1016/j.materresbull.2017.10.026
Received 28 August 2017; Received in revised form 11 October 2017; Accepted 15 October 2017
Available online 16 October 2017

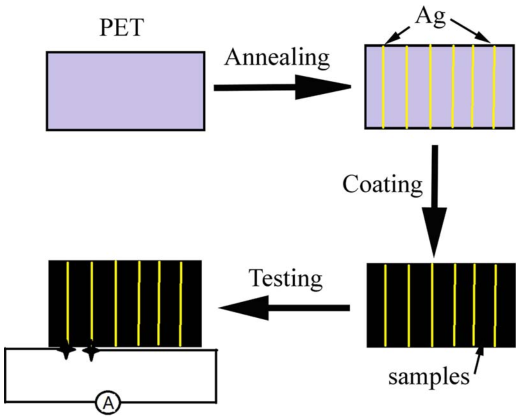

Scheme 1. Schematic illustration for the fabrication of the Bi_2S_3 flexible laser detector.

nanoflowers, the synthetic process was similar except that triethanolamine was used as the raw materials instead of ethylenediamine.

2.3. Material characterization

The structure of the Bi_2S_3 nanomaterials were investigated by X-ray power diffractometer (XRD, X'Pert PRO, PANalytical B.V., the Netherlands) with radiation of a Cu target (Ka, $\lambda = 0.15406$ nm) at 25 °C. Scanning electron microscopy (SEM, JSM-6701F) and transmission electron microscopy (TEM, JEM-2010) measurements were performed to study the morphology and microstructure. The UV–vis absorption spectra were recorded on a Shimadzu UV-3150 spectrophotometer. The photoresponse properties were measured under 808/980 nm laser and 500 W Xe-lamp light ($\lambda > 420$ nm), and with a Keithley 2410-C.

2.4. Fabrication of the flexible laser detectors

The flexible laser detector was fabricated by using the Bi_2S_3 nanorods and nanoflowers as the active materials and two parallel silver wires with an internal of 0.5 mm as the electrodes (see Scheme 1). The electrodes were deposited on the surface of the flexible polyethylene terephthalate (PET) substrate with the help of silver paste. A suitable amount of as-prepared Bi_2S_3 materials were dispersed in absolute ethanol solution containing small quantity of ethylene cellulose and terpineol to form uniform paste. Then the mixed materials paste was coated onto the PET substrate with Ag electrodes. After that, the PET device was dried in a vacuum oven at 80 °C for 3 h.

3. Result and discussion

Fig. 1a and b are the SEM images of the Bi_2S_3 crystals prepared by the polyol refluxing process. It reveals that the products consist of a large quantity of rod-like uniform nanostructures with typical length of 300–500 nm. As can be seen from Fig. 1b, the diameter of the Bi_2S_3 nanorods are about 30 nm. The typical SEM image of the as-prepared Bi_2S_3 nanoflowers is displayed in Fig. 1c and inset. It is observed that the surface of products is porous and each Bi_2S_3 nanoflowers is composed of dozens of flake-like nanopetals with the thickness of 20 ~ 30 nm. Further insight into the microstructural details of the flower-like architectures in Fig. 1d shows that those nanopetals interconnect with each other to form a porous structure. Moreover, the diffraction patterns presented in Fig. 1d inset reflected the relatively high crystallinity.

The phase and purity of the products are examined by the XRD pattern and the result is shown in Fig. 2a. It can be detected that all of the diffraction peaks can be well indexed to the pure orthorhombic Bi_2S_3 crystal with the lattice parameters of a = 1.1149 nm, b = 1.1304 nm, and c = 0.3981 nm, which match with the reported values (JCPDS Cards no. 17–0320). No peaks of any other phases, such as Bi_2O_3, BiOCl, are observed in the pattern, indicating the high purities of the samples. The absorption spectrum of the Bi_2S_3 nanorods and nanoflowers were further characterized by UV–3150. Fig. 2b displays two typical continuous broad absorptions in visible light and near-infrared area. In contrast, Bi_2S_3 nanoflowers sample has the same absorption between 200 nm to 890 nm and it exhibits more intensive absorption from 890 nm to 1100 nm compared to the Bi_2S_3 nanorods samples. Corresponding to the UV–vis absorption spectra, the energy band gaps of the Bi_2S_3 nanorods and nanoflowers were investigated by the formula $(\alpha h\nu)^2 = A(h\nu\text{-}E_g)$, where α, h, ν, A and E_g are the absorbance coefficient, planck constant, frequency of the incident light, characteristic constant, and the energy band gap, respectively. We can get the energy band gap values of both products are 1.49 eV and 1.63 eV, respectively, in good agreement with previous papers [21–23].

A good photoelectrical device must guarantee the convenience of

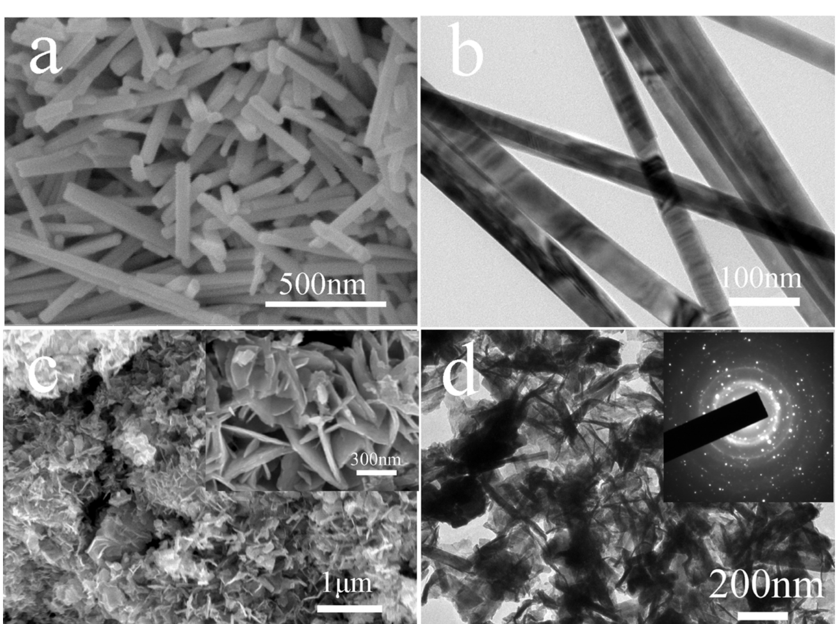

Fig. 1. (a, b) SEM images of the Bi_2S_3 nanorods, (c) SEM images and (d) TEM images of the Bi_2S_3 nanoflowers.